Proc. Natl. Acad. Sci. USA
Vol. 91, pp. 1014–1018, February 1994
Neurobiology

Critical roles of the S3 segment and S3–S4 linker of repeat I in activation of L-type calcium channels

(dihydropyridine receptor/heart/skeletal muscle)

JUNICHI NAKAI*†, BRETT A. ADAMS‡§, KEIJI IMOTO*, AND KURT G. BEAM‡¶

*Department of Medical Chemistry, Kyoto University Faculty of Medicine, Kyoto 606, Japan; and ‡Department of Physiology, College of Veterinary Medicine and Biomedical Sciences, Colorado State University, Fort Collins, CO 80523

Communicated by Bertil Hille, October 21, 1993 (received for review September 1, 1993)

ABSTRACT **Each of the four repeats (or motifs) of voltage-gated ion channels is thought to contain six transmembrane segments (S1–S6). Mutational analyses indicate that S4 functions as a voltage sensor and that the S5, S6, and S5–S6 linker contribute to formation of the ion pore. However, little information exists regarding the functional role(s) of the amino-terminal portion (S1–S3–S4 linker) of the repeats. Here we report that the amino acid composition of the S3 segment of repeat I and the linker connecting S3 and S4 segments of repeat I is critical for the difference in activation kinetics between cardiac and skeletal muscle L-type calcium channels. Mutant dihydropyridine receptors that have the skeletal muscle dihydropyridine receptor sequence in this region activated relatively slowly with the time constant of current activation (τ_{act}) > 5 ms, whereas mutants that have the cardiac counterpart there activated relatively rapidly with τ_{act} < 5 ms. Comparison of these two mutant groups indicates that a total of 11 conservative and 10 nonconservative amino acid changes from skeletal muscle to cardiac dihydropyridine receptor sequence are sufficient to convert activation from slow to fast. These data demonstrate a functional role for this region of voltage-gated ion channels.**

In cardiac muscle cells, L-type calcium channels activate rapidly; in contrast, these channels activate slowly in skeletal muscle cells (1). Previous analysis (2) of chimeras of the skeletal muscle and cardiac dihydropyridine receptors (DHPRs), which comprise the α_1 subunits of L-type calcium channels (3, 4), has revealed that when the first of the four homology repeats (repeat I) has cardiac sequence, activation is fast; conversely, when repeat I has skeletal muscle sequence, activation is slow. Identifying regions within repeat I that control activation kinetics may provide clues as to how the response of S4 to depolarization is coupled to channel activation. To this end, we have now expressed cDNAs encoding several "repeat I chimeras" in dysgenic (5, 6) myotubes, in which both excitation–contraction coupling and slow L-type calcium current are missing. Our results reveal that the amino acid composition of both the S3 segment of repeat I (IS3) and the linker connecting IS3 to the S4 segment of repeat I (IS4) is critical for the difference in activation kinetics between cardiac and skeletal muscle L-type calcium channels.

EXPERIMENTAL PROCEDURES

Preparation of Cells. Primary cultures of dysgenic (5, 6) myotubes were prepared from newborn mice essentially following described procedures (5, 7, 8). Briefly, myoblasts isolated from fore- and hindlimbs were plated at a density of 2×10^4 per 35-mm Falcon Primaria dish, on which a grid of ≈2-mm squares was ruled. After fusion of myoblasts into myotubes had begun, some cultures were treated for 24 hr with 10 μM cytosine arabinoside. The cultures were used within 6–9 days after plating cells.

Construction of DHPR cDNAs. To construct pCAC7, the nucleotides AAG (residues 493–495) of pCAC6 (8), the expression plasmid of the rabbit skeletal muscle DHPR used in our previous studies (2, 8–11), were replaced with the nucleotides CGC by site-directed mutagenesis (12). The compositions of the individual chimeric DHPRs are given below [Sk and Ca, skeletal muscle (13) and cardiac (14) DHPR, respectively; numbers in parentheses are amino acid numbers; for a region of identical sequence that flanks the joining site between the cardiac and skeletal muscle DHPRs, amino acid numbers are given as if that entire region were of cardiac sequence]: *SkC15* (2) Sk-(1–448), Ca-(571–787), Sk-(666–791), Ca-(923–1204), Sk-(1074–1129), Ca-(1261–1634), and Sk-(1510–1873). *SkC47* Ca-(1–222), Sk-(120–165), and Ca-(268–2171). Because all clones listed below have the same sequence as SkC15 except the region Sk-(1–448), only the differences from SkC15 are described: *SkC35* Sk-(1–165), Ca-(268–464), and Sk-(364–448); *SkC36* Sk-(1–55), Ca-(159–291), and Sk-(190–448); *SkC41* Sk-(1–136), Ca-(240–464), and Sk-(364–448); *SkC42* Sk-(1–55), Ca-(159–244), Sk-(142–165), Ca-(268–464), and Sk-(364–448); *SkC44* Sk-(1–85), Ca-(189–244), Sk-(142–165), Ca-(268–464), and Sk-(364–448); *SkC45* Sk-(1–55), Ca-(159–190), Sk-(88–165), Ca-(268–464), and Sk-(364–448); *SkC46* Sk-(1–55), Ca-(159–222), Sk-(120–165), Ca-(268–464), and Sk-(364–448). To make the chimeric cDNAs, four specific restriction sites were introduced into each of pCAC6 (8) and pCARD1 (9, 14) by site-directed mutagenesis (12). The substituted nucleotides with numbers (13, 14) are indicated as follows: SkC258 (cytosine-258), CaC567, G570 for *Xho* I; SkG348, CaG657 for *Mlu* I; SkA417, CaC724 for *Xba* I; and SkA522, A525 and CaA828, A831 for *Spe* I; these mutations do not affect any amino acid sequences. pSkC35 and pSkC36 have a *Spe* I site, pSkC41 and pSkC42 have *Xba* I and *Spe* I sites, pSkC44 and pSkC45 have *Xho* I, *Xba* I, and *Spe* I sites, and pSkC46 and pSkC47 have *Mlu* I, *Xba* I, and *Spe* I sites. Chimeric plasmids are composed of the following restriction fragments: *pSkC35*, *Spe* I (mutation site, Ca829)–*Sac* I(Ca957) from pCARD1, *Sac* I(Ca957)–*Bst*BI(Sk2175) from pCSk9 (2), *Bst*BI(Sk2175)–*Sal* I(vector) from pSkC15 (2), *Sal* I(vector)–*Spe* I(mutation site, Sk523) from pCAC6; *pSkC36*, *Bst*XI(Ca505)–*Spe* I(mutation site, Ca829) from

The publication costs of this article were defrayed in part by page charge payment. This article must therefore be hereby marked "*advertisement*" in accordance with 18 U.S.C. §1734 solely to indicate this fact.

Abbreviations: DHPR, dihydropyridine receptor; S1–S6, transmembrane segments 1–6, respectively; IS1–IS4, S1–S4 segments of repeat I, respectively.

†Present address: Department of Physiology, College of Veterinary Medicine and Biomedical Sciences, Colorado State University, Fort Collins, CO 80523.
§Present address: Department of Physiology and Biophysics, University of Iowa College of Medicine, 5-660 Bowen Science Building, Iowa City, IA 52242-1109.
¶To whom reprint requests should be addressed.

pCARD1, *Spe* I(mutation site, Sk523)–*Sac* I(Sk651) from pCAC6 and vector-containing *Sac* I(Sk651)–*Bst*XI(Sk196) from pSkC15; *pSkC41*, *Bst*XI(Sk196)–*Xba* I(mutation site, Sk415) from pCAC6, *Xba* I(mutation site, Ca724)–*Spe* I(mutation site, Ca829) from pCARD1 and vector-containing *Spe* I(mutation site, Ca829)–*Bst*XI(Sk196) from pSkC35; *pSkC42*, *Bst*XI(Ca505)–*Xba* I(mutation site, Ca724) from pCARD1, *Xba* I(mutation site, Sk415)–*Spe* I(mutation site, Sk523) from pCAC6, vector-containing *Spe* I(mutation site, Ca829)-*Bst*XI(Sk196) from pSkC35; *pSkC44*, *Bst*XI(Sk196)–*Xho* I(mutation site, Sk257) from pCAC6, *Xho* I(mutation site, Ca566)–*Xba* I(mutation site, Ca724) from pCARD1, *Xba* I(mutation site, Sk415)–*Sal* I(vector) from pSkC42 and *Sal* I(vector)–*Bst*XI(Sk196) from pSkC35; *pSkC45*, *Bst*XI-(Ca505)–*Xho* I(mutation site, Ca566) from pCARD1, *Xho* I(mutation site, Sk257)–*Spe* I(mutation site, Sk523) from pCAC6, and vector-containing *Spe* I(mutation site, Ca829)–*Bst*XI(Sk196) from pSkC35; *pSkC46*, *Bst*XI(Ca505)–*Mlu* I(mutation site, Ca654) from pCARD1, *Mlu* I(mutation site, Sk345)–*Spe* I(mutation site, Sk523) from pCAC6 and vector-containing *Spe* I(mutation site, Ca829)–*Bst*XI(Sk196) from pSkC35; *pSkC47*, *Hin*fI(Ca542)–*Bam*HI(Ca1265) from pSkC46 and vector-containing *Bam*HI(Ca1265)–*Hin*fI-(Ca542) from pCARD1.

Expression of cDNAs. Plasmids were introduced into nuclei of dysgenic myotubes by either microinjection (8) or the pricking method (15). With the pricking method, the culture medium was removed, and a group of suitable myotubes was submerged under 5 μl of plasmid at 1.0 μg/μl in TE buffer (10 mM Tris·HCl, pH 7.5/1 mM EDTA, pH 8.0). Nuclei of the submerged myotubes were then momentarily impaled with a fine micropipette mounted in an Olympus model IMT2-SYF injectoscope. Cells were cultured for an additional 1–4 days before electrophysiological measurements.

Electrophysiological Recordings. Calcium currents were measured by using the whole-cell variation of the patch-clamp technique as described (8). Holding potential was −80 mV. Test pulses were directly preceded by a 1-s prepulse to −30 mV to inactivate endogenous T-type calcium current (10). Calcium currents were corrected for linear components of capacitative and leak currents by digital scaling and subtraction of a control current elicited by a 20-mV hyperpolarization from the holding potential. This control current was also used to calculate the linear capacitance (C) for each cell. Patch pipettes contained 140 mM cesium aspartate, 10 mM Hepes, 10 mM Cs_2-EGTA, 5 mM $MgCl_2$ (pH 7.4 with CsOH). The bath contained 10 mM Ca^{2+}, 145 mM tetraethylammonium ion, 165 mM Cl^-, 10 mM Hepes, 0.003 mM tetrodotoxin (pH 7.4 with CsOH). Temperature was 20–23°C.

RESULTS

The cDNA for the rabbit skeletal muscle DHPR exhibits a polymorphism such that residue 165 of the IS4 segment is either lysine or arginine (13). A lysine is encoded at this position by pCAC6 (8), the expression plasmid that we had previously used for the skeletal muscle DHPR (2, 8–11), whereas an arginine is encoded at the corresponding position (residue 267) by pCARD1 (9, 14), the expression plasmid used in our studies of cardiac DHPR (2, 9–11). Except for this residue, pCAC6 and pCARD1 encode IS4 segments having identical amino acid sequences. To investigate the importance of this single amino acid difference, we constructed pCAC7 (see *Experimental Procedures*), which encodes Arg-165 but is otherwise identical to pCAC6. Fig. 1 shows that the calcium current activation kinetics are slow for both CAC6 and CAC7 DHPRs. The time constant of current activation (τ_{act}) (2), measured at a test potential (V_{test}) near the peak of the current–voltage relation, was 53.4 ± 10.4 ms (mean ± SD) for CAC6 (n = 10) and 39.2 ± 22.2 ms for CAC7 (n = 14).

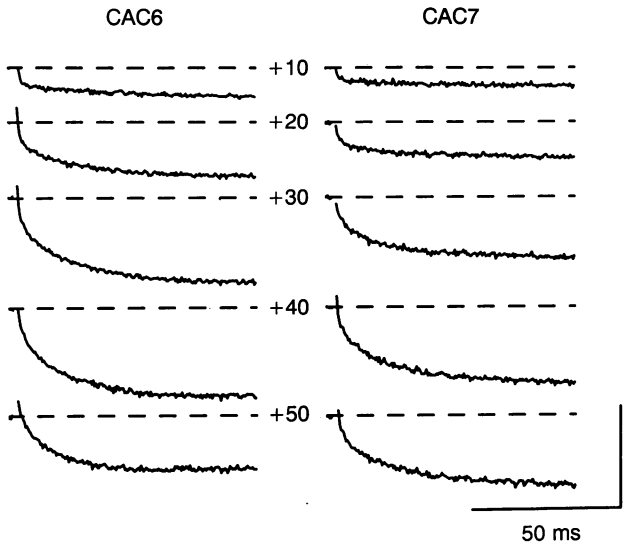

FIG. 1. Comparison of calcium currents produced by the skeletal muscle DHPRs CAC6 (Lys-165) and CAC7 (Arg-165) in dysgenic myotubes. Test potentials are indicated next to the current traces (vertical calibration = 3 nA). For CAC6 (cell BR45) linear capacitance (C) was 625 pF: for CAC7 (cell BV53) C was 455 pF. The test potential at which calcium conductance was half-maximal (V_G) was 25.9 ± 4.0 mV (n = 9) and 32.1 ± 7.3 mV (n = 10) for CAC6 and CAC7, respectively.

Because the single amino acid difference in IS4 did not determine whether activation kinetics were slow or fast, we constructed cDNAs encoding eight repeat I chimeras (SkC35, SkC36, SkC41, SkC42, SkC44, SkC45, SkC46, and SkC47). Fig. 2 illustrates each of these chimeras schematically, together with a representative calcium current produced by expression of that chimera in a dysgenic myotube. SkC15, in which repeat I has entirely skeletal muscle sequence, was used as the parental structure because it produces slowly activating current (2).

We initially compared activation kinetics of SkC36 and SkC35 in which, respectively, either the amino-terminal or carboxyl-terminal half of repeat I of SkC15 was replaced by the corresponding cardiac sequence. SkC35 activated slowly, whereas SkC36 activated rapidly (Fig. 2). This result indicates that the identity of the amino-terminal half of repeat I [the region beginning with segment 1 of repeat I (IS1) and ending with the IS3–IS4 linker] determines whether activation is slow or fast. We next examined SkC41 and SkC42, in which complementary regions of the amino-terminal half of repeat I were converted from skeletal muscle to cardiac sequence (Fig. 2). Comparison of SkC35 and SkC41 chimeras reveals that conversion of the IS3–IS4 linker from skeletal muscle to cardiac sequence changed the current from slowly to rapidly activating. Thus, the skeletal muscle IS3–IS4 linker is necessary for slow activation. However, it is not sufficient because slowly activating current is not produced by SkC42 chimera, in which only the IS3–IS4 linker is skeletal muscle in origin.

To examine the possibility that activation kinetics might be determined by interactions between the IS3–IS4 linker and other regions of repeat I, we tested SkC44, SkC45, and SkC46. SkC44, in which IS1 and the putatively extracellular IS1–IS2 and IS3–IS4 linkers have skeletal muscle sequence, produced rapidly activating current. In contrast, SkC45, in which IS2, the IS2–IS3 linker, IS3, and the IS3–IS4 linker all have skeletal muscle sequence, produced slowly activating current. Slow activation was also produced by SkC46, in which only IS3 and the IS3–IS4 linker have skeletal muscle sequence. Furthermore, slow activation kinetics do not require any other portion of the DHPR to have skeletal muscle

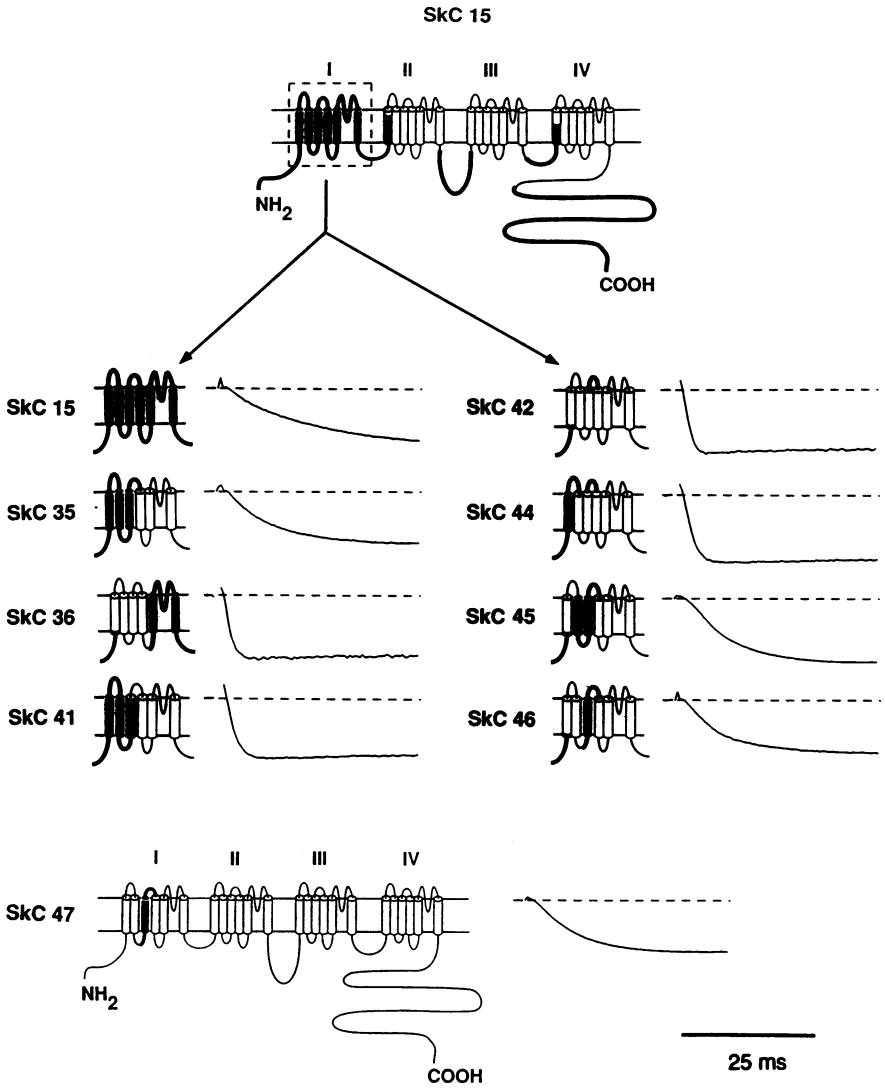

FIG. 2. Schematic representation of repeat I chimeras and the calcium currents resulting from their expression in dysgenic myotubes. Regions of the chimeric DHPRs having skeletal muscle sequence are represented by thick lines and filled cylinders, and regions having cardiac sequence are represented by thin lines and open cylinders, where the cylinders indicate putative transmembrane segments, and the lines indicate linking regions. For all constructs except SkC15 (2), IS4 is represented by an empty cylinder because it is identical for the cardiac and skeletal muscle DHPRs, except for the polymorphism (lysine or arginine) at residue 165 of the skeletal muscle DHPR, which is unimportant for activation kinetics (see *Results* and Fig. 1). SkC36 and SkC41 have an arginine at the corresponding position; all the other chimeras have a lysine at this position. SkC15 (at top) was used as the parent structure; the boxed region indicates repeat I, portions of which were replaced with the corresponding sequence from CARD1 to produce the chimeric DHPRs SkC35, SkC36, SkC41, SkC42, SkC44, SkC45, and SkC46. For these constructs, only repeat I is diagrammed; the remainder of each chimeric DHPR corresponds to SkC15. For SkC47 (at bottom), CARD1 was used as the parent structure. The illustrated calcium currents were recorded near the peak of the current–voltage relation. Data were as follows: SkC15 (cell BV33)—C = 200 pF, test potential (V_{test}) = +20 mV, maximum inward current for illustrated trace (I_{max}) = 3.84 nA; SkC35 (cell BR09)—C = 440 pF, V_{test} = +20 mV, I_{max} = 8.01 nA; SkC36 (cell BR38)—C = 340 pF, V_{test} = +30 mV, I_{max} = 2.77 nA; SkC41 (cell BR74)—C = 100 pF, V_{test} = +30 mV, I_{max} = 2.76 nA; SkC42 (cell BR96)—C = 210 pF, V_{test} = +20 mV, I_{max} = 3.63 nA; SkC44 (cell BT74)—C = 640 pF, V_{test} = +20 mV, I_{max} = 5.86 nA; SkC45 (cell BT60)—C = 225 pF, V_{test} = +10 mV, I_{max} = 11.88 nA; SkC46 (cell BT54)—C = 280 pF, V_{test} = +10 mV, I_{max} = 6.15 nA; SkC47 (cell BV50)—C = 610 pF, V_{test} = 0 mV, I_{max} = 23.91 nA.

sequence, as demonstrated by SkC47, which has entirely cardiac sequence, except for IS3 and the IS3–IS4 linker. Thus, in our experiments, IS3 and the IS3–IS4 linker represent the minimum determinants of slow activation by the skeletal muscle DHPR.

Fig. 3 summarizes values of τ_{act} determined by single-exponential fits to the currents produced by the repeat I chimeras. The data can be divided into two groups with no overlap: SkC15, SkC35, SkC45, SkC46, and SkC47 all activated relatively slowly, with $\tau_{act} > 5$ ms, whereas SkC36, SkC41, SkC42, SkC44, and CARD1 all activated relatively rapidly, with $\tau_{act} < 5$ ms. As exemplified by SkC47, all the DHPRs in the slowly activating group have skeletal muscle sequence for IS3 and the IS3–IS4 linker (Fig. 2).

The voltage-dependence of calcium channel activation can be characterized by a slope factor (k) and the test potential (V_G) eliciting half-maximal activation of calcium channel conductance. Table 1 summarizes values of V_G and k for myotubes with a maximum calculated voltage error (10) of <10 mV. From Table 1, it is evident that there was no consistent relationship between activation rate and the voltage-dependence of steady-state activation.

DISCUSSION

Over the last several years, work in a number of laboratories on sodium, potassium, and calcium channels has contributed to an emerging picture of the role played by specific regions

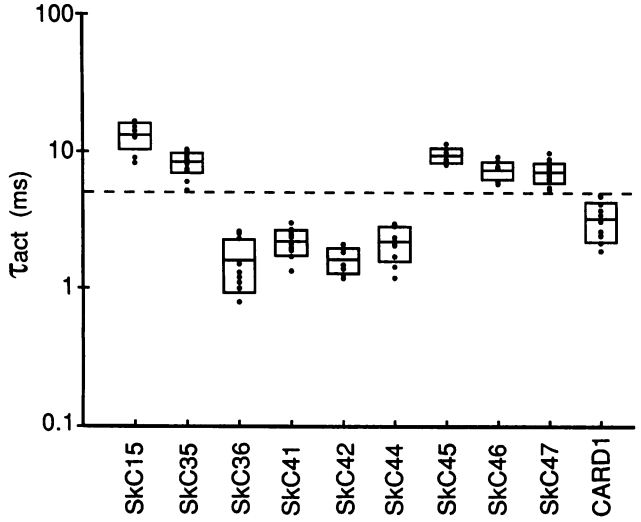

FIG. 3. Time constant of activation (τ_{act}) for calcium currents generated by DHPRs in dysgenic myotubes. Individual data points are plotted as filled circles (overlapping values are plotted as single points), the short horizontal line indicates the mean, and the box indicates ±SD. The dashed horizontal line is drawn at 5 ms. Values of τ_{act} were determined for each myotube by fitting the activation phase of current according to $I(t) = I_\infty[1 - \exp(-t/\tau_{act})]$, where $I(t)$ is the current at time t after "stepping" membrane potential to the test potential (V_{test}), I_∞ is the steady-state current, and V_{test} was equal, or 10 mV positive, to the potential eliciting maximal inward current. This V_{test} was used as the standard for comparing different constructs to eliminate kinetic differences arising from cell-to-cell and construct-to-construct (Table 1) variability in voltage-dependence of activation. However, the data also fell cleanly into two groups when comparisons were made at strongly depolarized test potentials where the rate of activation was little affected by differences in voltage-dependence of activation: τ_{act} = 13.1 ± 2.8 ms (n = 9), 8.4 ± 1.4 ms (n = 18), 1.6 ± 0.7 ms (n = 13), 2.2 ± 0.5 ms (n = 12), 1.6 ± 0.3 ms (n = 9), 2.2 ± 0.6 ms (n = 10), 9.5 ± 1.2 ms (n = 8), 7.3 ± 1.1 ms (n = 12), 7.1 ± 1.2 ms (n = 20), and 3.2 ± 1.0 ms (n = 11), respectively, for DHPRs in the order indicated along the abscissa.

in gating and selective ion permeation. Mutations of the S4 segment (16–20), the S4–S5 linker (20, 21), and the S5 segment (20) have been found to affect the voltage dependence of activation. The S5 segment, the S5–S6 linker, and the S6 segment are thought to contribute to the ion-selective pore (22), and the IIIS5–IIIS6 linker, IIIS6, and IVS6 are thought to compose the dihydropyridine-binding site of

Table 1. Voltage-dependence for activation of chimeric calcium channels

DHPR	Activation rate	$\overline{V}_G$, mV	k, mV	G_{max}, nS·nF^{-1}	n
SkC15	Slow	4.2 ± 5.1	5.4 ± 1.5	414 ± 176	6
SkC35	Slow	10.3 ± 4.9	5.6 ± 0.7	530 ± 235	10
SkC36	Fast	15.6 ± 3.5	6.9 ± 1.3	281 ± 126	9
SkC41	Fast	11.5 ± 5.3	6.3 ± 0.9	344 ± 146	11
SkC42	Fast	11.0 ± 3.7	7.1 ± 1.4	217 ± 50	5
SkC44	Fast	−2.5 ± 5.3	5.8 ± 0.7	222 ± 76	6
SkC45	Slow	1.5 ± 11.0	5.7 ± 0.8	535 ± 165	6
SkC46	Slow	2.9 ± 5.8	5.9 ± 1.5	256 ± 75	12
SkC47	Slow	−0.8 ± 3.2	8.0 ± 1.2	626 ± 153	14
CARD1	Fast	5.1 ± 5.9	7.7 ± 1.1	499 ± 133	8

Data are given as mean ± SD. Values of $\overline{V}_G$, the potential for activation of half-maximal conductance; k, a slope factor; and G_{max}, the maximal calcium conductance, were obtained by fitting measured currents according to $I = G_{max}(V - V_{rev})/\{1 + \exp[-(V - \overline{V}_G)/k]\}$, where I is the peak calcium current activated at test potential V, and V_{rev} is the extrapolated reversal potential. n, Number of myotubes tested.

L-type calcium channels (23). Thus, the carboxyl-terminal half (S4–S6) of the repeats are involved in determining voltage dependence, ionic permeation, and drug-binding sites of the channels. In contrast, before the present work, no function had yet been ascribed to S1, S2, S3, and the S3–S4 linker. Our results demonstrate that differences in the amino acid sequence of IS3 and the IS3–IS4 linker are critical for the difference in current kinetics between the cardiac and skeletal muscle DHPRs, suggesting that this region plays a hitherto unknown role in channel activation.

Clearly, activation kinetics are not governed only by the IS3 segment and IS3–IS4 linker. For example, the rate of activation is affected by current density (24). Additionally, the L-type calcium channel exists as a complex of α_1, α_2/δ, β, and γ subunits (3, 4), and the β subunit has been shown to affect the rate of activation (25–32). There is a possibility that the identity of the IS3–IS4 linker alters the interaction of the DHPR (= α_1 subunit) with an endogenous β subunit in dysgenic myotubes. However, the β subunit is thought to interact with cytoplasmic portions of the DHPR (33, 34). Additionally, converting only the IS3–IS4 linker from skeletal to cardiac sequence was sufficient to change activation from slow to fast (compare SkC35 and SkC41 in Fig. 2). If altered β subunit interactions are to account for this kinetic change, it would mean that an intracellular interaction is

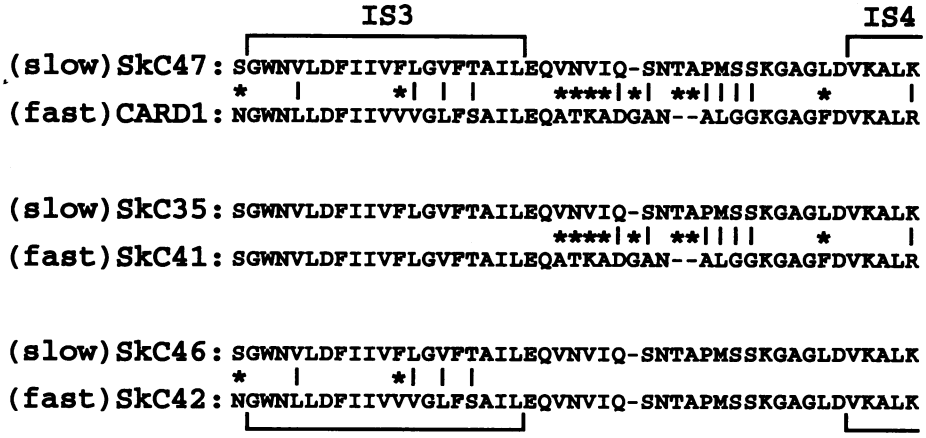

FIG. 4. Comparison of the IS3–IS4 regions (one-letter amino acid code) of six different DHPRs that produced fast or slow activation as indicated. Between the paired sequences, conservative amino acid changes are indicated by vertical lines, and nonconservative changes are indicated by asterisks. Dashes represent gaps introduced to align the sequences, and brackets delimit the putative segments IS3 and IS4. For each pair of constructs, the sequences are identical for regions not shown. The illustrated sequences for SkC47, SkC35, and SkC46 coincide with that of CAC6 (8, 13), extending from Ser-120 (S120) to K165, and the sequence for CARD1 (9, 14) extends from N223 to R267.

controlled by the identity of a small segment that is thought to be extracellular. It should also be noted that heterologous expression demonstrates that skeletal muscle and cardiac DHPRs can function in isolation as calcium channels, exhibiting slow and fast activation, respectively (35, 36). Thus, the simplest explanation for our results is that the kinetic differences between the repeat I chimeras are intrinsic to the DHPR (α_1 subunit) itself.

Fig. 4 compares the sequences of IS3 and the IS3–IS4 linker for different constructs having either slow or fast activation. Comparison of SkC47 and CARD1 indicates that a total of 11 conservative (vertical lines) and 10 nonconservative (asterisks) amino acid changes are sufficient to convert activation from slow to fast; eight of the 10 nonconservative changes are in the IS3–IS4 linker. However, it is the identity of both IS3 and the IS3–IS4 linker that appears important because changing either IS3 (SkC46 vs. SkC42) or the IS3–IS4 linker (SkC35 vs. SkC41) from skeletal muscle to cardiac sequence converts activation from slow to fast. Interactive effects of these two regions could be explained in many ways. One possibility is that the IS3–IS4 linker folds into the membrane, thus allowing amino acids of the linker to interact directly with amino acids of IS3.

Proposal of a detailed functional model for IS3 and the IS3–IS4 linker is premature at this time, but two possibilities are immediately apparent. One possibility is that this region affects the rate at which S4, the putative voltage sensor (16–20), responds to a change in membrane potential. However, measurements of immobilization-resistant charge movement suggest that the voltage sensors of skeletal muscle and cardiac DHPRs respond similarly to voltage (10). Moreover, among the repeat I chimeras, there was no consistent relationship between the activation rate and the voltage dependence of steady-state activation (Table 1). Thus, IS3 and the IS3–IS4 linker may instead influence channel-opening conformational changes that occur only after the voltage sensor has responded to depolarization.

We acknowledge the late Prof. Shosaku Numa for his encouragement and support for this project. We thank Drs. T. Tanabe and R. Dirksen for helpful discussion and M. Kuchiishi and N. Nakamura for excellent technical help. We also thank L. Bennett, A. Beam, and J. Hanneman for providing cultured myotubes. This research was supported, in part, by the Ministry of Education, Science and Culture of Japan, the Institute of Physical and Chemical Research and by the U.S. National Institutes of Health.

1. Bean, B. P. (1989) *Annu. Rev. Physiol.* **51**, 367–384.
2. Tanabe, T., Adams, B. A., Numa, S. & Beam, K. G. (1991) *Nature (London)* **352**, 800–803.
3. Catterall, W. A. (1988) *Science* **242**, 50–61.
4. Campbell, K. P., Leung, A. T. & Sharp, A. H. (1988) *Trends Neurosci.* **11**, 425–430.
5. Beam, K. G., Knudson, C. M. & Powell, J. A. (1986) *Nature (London)* **320**, 168–170.
6. Chaudhari, N. (1992) *J. Biol. Chem.* **267**, 25636–25639.
7. Beam, K. G. & Knudson, C. M. (1988) *J. Gen. Physiol.* **91**, 781–798.
8. Tanabe, T., Beam, K. G., Powell, J. A. & Numa, S. (1988) *Nature (London)* **336**, 134–139.
9. Tanabe, T., Mikami, A., Numa, S. & Beam, K. G. (1990) *Nature (London)* **344**, 451–453.
10. Adams, B. A., Tanabe, T., Mikami, A., Numa, S. & Beam, K. G. (1990) *Nature (London)* **346**, 569–572.
11. Tanabe, T., Beam, K. G., Adams, B. A., Niidome, T. & Numa, S. (1990) *Nature (London)* **346**, 567–569.
12. Sayers, J. R. & Eckstein, F. (1989) in *Protein Function: A Practical Approach*, ed. Creighton, T. E. (IRL, Oxford), pp. 279–295.
13. Tanabe, T., Takeshima, H., Mikami, A., Flockerzi, V., Takahashi, H., Kangawa, K., Kojima, M., Matsuo, H., Hirose, T. & Numa, S. (1987) *Nature (London)* **328**, 313–318.
14. Mikami, A., Imoto, K., Tanabe, T., Niidome, T., Mori, Y., Takeshima, H., Narumiya, S. & Numa, S. (1989) *Nature (London)* **340**, 230–233.
15. Yamamoto, F., Furusawa, M., Furusawa, I. & Obinata, M. (1982) *Exp. Cell Res.* **142**, 79–84.
16. Stühmer, W., Conti, F., Suzuki, H., Wang, X., Noda, M., Yahagi, N., Kubo, H. & Numa, S. (1989) *Nature (London)* **339**, 597–603.
17. Auld, V. J., Goldin, A. L., Krafte, D. S., Catterall, W. A., Lester, H. A., Davidson, N. & Dunn, R. J. (1990) *Proc. Natl. Acad. Sci. USA* **87**, 323–327.
18. Papazian, D. M., Timpe, L. C., Jan, Y. N. & Jan, L. Y. (1991) *Nature (London)* **349**, 305–310.
19. Lopez, G. A., Jan, Y. N. & Jan, L. Y. (1991) *Neuron* **7**, 327–336.
20. McCormack, K., Tanouye, M. A., Iverson, L. E., Lin, J.-W., Ramaswami, M., McCormack, T., Campanelli, J. T., Mathew, M. K. & Rudy, B. (1991) *Proc. Natl. Acad. Sci. USA* **88**, 2931–2935.
21. Isacoff, E. Y., Jan, Y. N. & Jan, L. Y. (1991) *Nature (London)* **353**, 86–90.
22. Miller, C. (1992) *Curr. Biol.* **2**, 573–575.
23. Striessnig, J., Murphy, B. J. & Catterall, W. A. (1991) *Proc. Natl. Acad. Sci. USA* **88**, 10769–10773.
24. Adams, B. A. & Beam, K. G. (1992) *Biophys. J.* **61**, A419 (abstr.).
25. Varadi, G., Lory, P., Schultz, D., Varadi, M. & Schwartz, A. (1991) *Nature (London)* **352**, 159–162.
26. Wei, X., Perez-Reyes, E., Lacerda, A. E., Gabriele, S., Brown, A. M. & Birnbaumer, L. (1991) *J. Biol. Chem.* **266**, 21943–21947.
27. Lacerda, A. E., Kim, H. S., Ruth, P., Perez-Reyes, E., Flockerzi, V., Hofmann, F., Birnbaumer, L. & Brown, A. M. (1991) *Nature (London)* **352**, 527–530.
28. Singer, D., Biel, M., Lotan, I., Flockerzi, V., Hofmann, F. & Dascal, N. (1991) *Science* **253**, 1553–1557.
29. Hullin, R., Singer-Lahat, D., Freichel, M., Biel, M., Dascal, N., Hofmann, F. & Flockerzi, V. (1992) *EMBO J.* **11**, 885–890.
30. Perez-Reyes, E., Castellano, A., Kim, H. S., Bertrand, P., Baggstrom, E., Lacerda, A. E., Wei, X. & Birnbaumer, L. (1992) *J. Biol. Chem.* **267**, 1792–1797.
31. Castellano, A., Wei, X., Birnbaumer, L. & Perez-Reyes, E. (1993) *J. Biol. Chem.* **268**, 12359–12366.
32. Castellano, A., Wei, X., Birnbaumer, L. & Perez-Reyes, E. (1993) *J. Biol. Chem.* **268**, 3450–3455.
33. Lory, P., Varadi, G. & Schwartz, A. (1992) *Biophys. J.* **63**, 1421–1424.
34. Ruth, P., Röhrkasten, A., Biel, M., Bosse, E., Regulla, S., Meyer, H. E., Flockerzi, V. & Hofmann, F. (1989) *Science* **245**, 1115–1118.
35. Perez-Reyes, E., Kim, H. S., Lacerda, A. E., Horne, W., Wei, X., Rampe, D., Campbell, K. P., Brown, A. M. & Birnbaumer, L. (1989) *Nature (London)* **340**, 233–236.
36. Yoshida, A., Takahashi, M., Nishimura, S., Takeshima, H. & Kokubun, S. (1992) *FEBS Lett.* **309**, 343–349.